

AN EVALUATION OF INFLATABLE TRUSS FRAME FOR SPACE APPLICATIONS

D. K. Darooka¹
S. E. Scarborough²
D. P. Cadogan³

Research and Technology Department
ILC Dover, Inc; Frederica DE

Abstract

NASA has been evaluating several very large space solar power (SSP) system concepts with a varying degree of configurations. A key to successful deployment of these very large-scale systems lies in meeting their structural needs. The structures that will support the SSP system requirements will, thus, be extremely large compared to current standards. These structures must meet the requirements of extremely low mass, low packaging volume and be capable of controlled deployment. A breakthrough in the current state-of-the-art of the structural booms is required to meet these diverse requirements. To meet this goal several boom concepts, which have the potential to be deployable to very long lengths, are under consideration for their structural and volume packaging efficiencies. Different current and potential structural concepts were compared for their structural efficiency to meet the desired loading expected in typical space missions. From this analysis a truss frame boom was found to be very mass efficient for very long length booms. This truss frame was configured into a unique space inflatable structure known as the Inflatable Space Frame (ISF). This structure was designed and built using a shape memory polymer as matrix and graphite as the reinforcement to achieve the

foldability and deployability. The structural efficiency and the foldability of the truss structure impart conflicting requirements upon the composite materials. Both were, however, achieved by properly balancing the load distribution among various truss members and selecting proper fiber orientation. The test results showed performance comparable to or better than the current state-of-the-art and verified the design methodology used. Several key technical challenges were also overcome while fabricating the truss frame structure. This paper discusses the comparative merit, analysis, design, development and testing of a prototype ISF.

Introduction

NASA has been investigating space-based solar power generating systems that would deliver the collected power to terrestrial markets. A driving factor for the realization of this system is significant advances in multiple space-related technologies. These technologies then in turn can be used to develop new system concepts for the SSP project.

In this regard a critical challenge is to develop large, ultra-lightweight deployable structures. NASA is currently evaluating several different potential structural concepts. In addition to very long boom structures, various support structures are required which consist of boom elements. Many studies have been and are being conducted in identifying such ultra-lightweight structures under various projects sponsored by NASA and other agencies. The development of the Inflatable Space Frame, as described in the following

¹ Key Technologist

² Process Engineer

³ Sr. Design Engineer

Copyright © 2001 by the American Institute of Aeronautics and Astronautics, Inc. All rights reserved.

sections, is a significant step forward in providing the structural elements for the SSP program and other gossamer applications. The inflatable truss structure that has been fabricated and tested demonstrates the validity of the concept and can also be used to identify specific areas for future development.

Inflatable Truss Frame Structure

A typical truss frame structure consists of longerons, which are interconnected by diagonals and batten members. Longerons, which are the primary load bearing elements, are sized to meet the axial and bending stiffness requirements. Diagonals are sized to meet shear and torsion requirements. Battens, which do not carry any load, serve to stabilize the structure and maintain the cross-section under small inertial and external loads. The high moment of inertia is achieved by the longerons, which makes the structure stronger and stiffer. Thus, batten and diagonal members primarily constitute parasitic mass of the structure, which is primarily loaded in the axial direction. For the same reason this structure is primarily suited for longer lengths at higher loads where the relative contribution of the parasitic mass is lower. Given the arrangement of individual members of the truss, it is less vulnerable to circumferential buckling which has been observed in many monocoque thin wall structures. Similarly, the ratio of tube radius to wall thickness, which relates to manufacturing imperfection, is less critical in the truss structures as the individual tube radius is very small.

There are many ways in which the longerons can be arranged to form the truss structure. Two of the most common arrangements are shown in Figure 1. In the

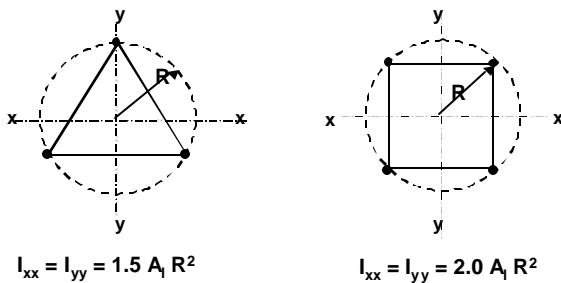


Figure 1 Potential Truss Configurations

first case, three longerons form an equilateral triangle and in the second case four longerons form a square cross-section. It is seen that the square configuration with four longerons gives higher moment of inertia for the same A_l (cross-sectional area of the longeron) and R . However, as seen from Figure 2, on a specific stiffness basis, the benefit of the square configuration vanishes with increasing length. Further, a triangular configuration has less number of joints and piece parts making it more reliable. Accordingly, a three-longeron configuration was selected for this study.

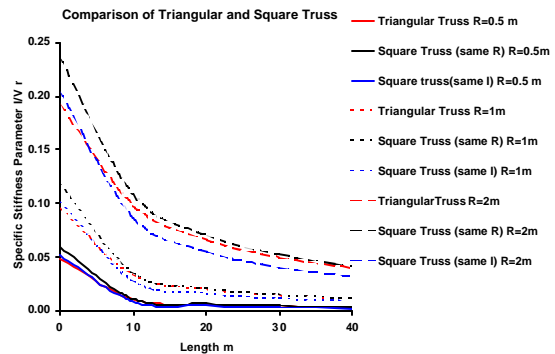


Figure 2 Specific stiffness of triangular and square truss configuration

The overall Inflatable space frame boom concept consists of a rigidizable truss frame, as described above, that is enclosed by and attached to a circumferential film of Kapton™ as shown in Figure 3. The Kapton™ film serves as an inflatable tube that is used to deploy the structure and provides the required tension to form the shape prior to rigidization. The shape formation is augmented by the shape memory effect of the matrix material used. The truss itself is made of small hollow tubes that are connected at the intersection. The entire structure can be collapsed as shown in the figure by heating above the glass transition temperature (T_g) of the matrix material. Once it is collapsed it can be rolled while still above T_g on to a roller for stowage into the spacecraft. This way embedded heaters are avoided and reversible and controlled rigidization is possible. These aspects of the concept will be discussed in more detail in the subsequent paragraphs.

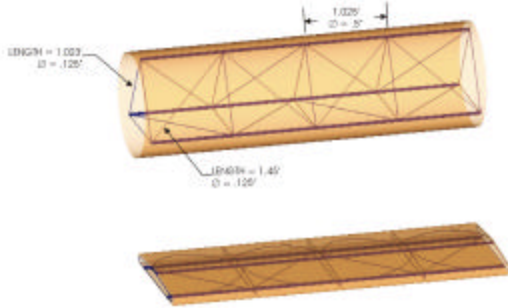


Figure 3 ISF structure concept

Material Considerations

Composite Materials

The stiffness of the composite material from which the tubes are made is dominated by the fibers. Thus, volume fraction of the fibers in the composite material is the most critical parameter for improving the modulus of elasticity. In this sense a unidirectional composite material, where all the fibers are oriented in one direction, would achieve the highest volume fraction and hence the highest modulus of elasticity. In practice, the maximum volume fraction is 60% in unidirectional aligned fiber composites. The desirable fiber volume fraction, in reality, is limited to a much lower value due to the requirement of foldability, which has a deleterious effect on the fiber strength. This, in principle, could impose a serious compromise on the achievable modulus of elasticity.

Stiffness can also be improved by minimizing the tows in the normal direction, which minimizes the waviness of the longitudinal tows. However, some tows in the hoop (fill) direction are required to maintain the overall integrity of the tubular structure, which limits the volume fraction in the given direction and hence the achievable modulus of elasticity. Another factor that could increase the stiffness is the number of plies used in the composite material which increases the thickness and hence the moment of inertia. This, of course, also increases the mass. Therefore, again necessitating a compromise. A micromechanics analysis was used to optimize the constitution of the composite

material to achieve the optimum stiffness vs. mass results.

Candidate Fiber Materials

Two candidate fiber materials that offer the highest modulus among those easily available and suitable for the current application include graphite and Kevlar™. The modulus of graphite fibers can be as high as 75 Msi. However, higher the modulus more brittle they become. Thus, folding of the fibers without breakage becomes difficult. Typically, for applications where folding of the fibers is a definite possibility for stowing, graphite fibers of modulus 33.5 Msi are selected. This is still very high compared to other available fibers. Graphite also has other advantages, which include its higher thermal and electrical conductivity, both very important in space application. Its long-term resistance to the space environment is also well known. Graphite was therefore selected for the truss structure in the current study.

Kevlar™, which is an aramid fiber with a modulus approximately 65% and density approximately 90% of the graphite fibers, was also considered. In addition to its lower modulus, the key disadvantages of Kevlar™ are its lower thermal and electrical conductivity and sensitivity to the space environment. However, for the reason that it has lower modulus and higher toughness it offers greater potential for foldability without breakage. Thus, Kevlar™ can be effectively used for batten and diagonal members which require lower modulus and have a smaller bend radius compared to the longerons. Similarly, Kevlar™ could be a good choice for the joints to achieve additional flexibility in this area. A hybrid graphite/Kevlar™ truss structure has the potential to substantially improve the overall performance of the structure.

Candidate Matrix Materials

Essentially there are two kinds of polymers available for consideration as matrix material. These include thermoset and thermoplastic polymers.

In a thermoset polymer the molecules are chemically joined together by

cross-links forming a rigid, 3-D network structure. Once these cross-links are formed during the curing reaction the thermoset polymer can not be melted and reshaped (post-formed) by the application of heat and pressure. However, if the number of cross-links is low, it may still be possible to soften them at elevated temperature.

In a thermoplastic polymer, on the other hand, individual molecules are linear in structure with no chemical linking between them. They are held in place by weak secondary bonds (intermolecular forces). With the application of heat and pressure, these intermolecular bonds in a solid thermoplastic polymer can be temporarily broken and the molecules can be moved relative to each other to flow into a new position. Upon cooling, the molecules freeze in their new positions, restoring the secondary bonds between them, resulting in a new solid shape.

Resulting from this distinctly different behavior of the two polymers are several characteristics, which set them apart for suitability to space inflatable and rigidizable structures. For example, rigidization of a thermoset polymer is non-reversible. It also requires longer rigidization time and has limited storage life. Because of its relatively high modulus it undergoes lower strain to failure and therefore has lower impact resistance. It is, however, thermally and chemically more stable and exhibits less creep and stress relaxation. Thermoplastics, on the other hand, have relatively lower modulus and hence higher strain to failure, which makes them resistant to microcracking and impact. Thermoplastics also have unlimited storage life at room temperature and because they do not exhibit tackiness they are easier to handle. The most important property of thermoplastics is their shape memory behavior, which can be effectively utilized in space deployment. The glass transition temperature (T_g) associated with this property, however, must be above the maximum expected orbital temperature.

It is clear that a balance of characteristics between the two candidate matrix materials would lead to an ideal solution. ILC Dover, Inc has developed a proprietary epoxy thermoplastic resin, which

provides the balance of these properties. This resin has been used in the current study.

Thermoplastic Shape Memory Behavior

The basic principles of shape memory effect in thermoplastics can be well described by reference to Figure 4. The permanent shape is given to the material when it is first heated above its curing temperature with the constraint of the permanent shape applied and then rapidly cooled in-situ. This is the lowest stress condition. Subsequently stress energy can be applied either by cold deformation or by constrained heating above the T_g . If the material is heated above the T_g with the constraint of the new shape and then cooled below the T_g it acquires this new temporary shape. Constrained heating can change this shape ad infinitum. If the material is heated above the T_g , but unconstrained, it releases the stored energy and reverts back to the permanent shape. For space application, the T_g must be above the maximum orbital temperature to prevent unintended loss of shape under orbital forces. Typical orbit temperature in low earth orbit is less than 50°C and the T_g can be tailored to some extent so that the T_g is above 50°C . It is however desirable to keep the T_g as low as possible as the heating power required goes up with the temperature.

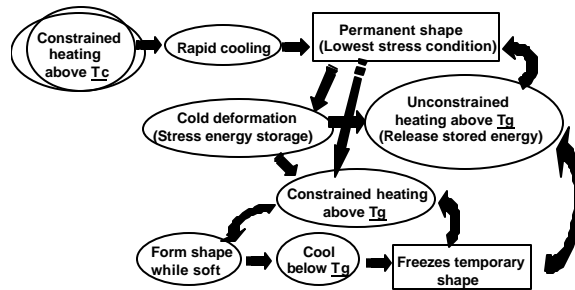


Figure 4 Shape memory behavior of thermoplastics

Packaging and Deployment

The Inflatable Space frame (ISF) is designed to be collapsible so that it can be packaged into a small volume to facilitate integration into a launch vehicle. The truss assembly formation and deployment using the shape memory effect of the thermoplastics is shown in Figure 5. In the

figure each step is identified by the number, which also depicts the number of times the structure undergoes shape change until permanently deployed in space. Each step curve, although shown separately for clarity, are actually closely overlapping. Curing the material inside the molds at the curing temperature, and subsequently cooling it while still inside the mold, forms individual tubes as shown by process 1. After the truss is assembled using individual tubes formed in this fashion, it is again heated past the T_g to give it the shape of the stowed configuration (process 2), and then frozen in shape by cooling below T_g (process 3). When ready to deploy in space the entire stowed configuration is brought to temperature greater than T_g (process 4) and continued to deploy while still above T_g . The structure is subsequently cooled below T_g while unconstrained and the shape is locked in place.

One possible deployment sequence is shown schematically in Figure 6. In the diagram shown, the truss structure is rolled inside a stowage cavity that has means for internal heating and is thermally insulated. The stowage cavity, which is attached to the spacecraft for launch, also has an extendable heater that keeps the structure above T_g as it is being deployed. The deployment begins from the spacecraft end by inflating the surrounding shroud by a gas stored inside the spacecraft. Simultaneous heating and deployment assures positive truss configuration. Inflation of the shell tensions the frame at points where it is attached to the frame causing it to take the global shape. At the same time heating above T_g triggers the shape memory of the individual truss members and causes them to extend and take the circular cross-sectional shape. The key advantage of the shape memory over other concepts can be easily seen here; it avoids having to individually pressurize the tubes to form their required configuration. Another advantage of using thermoplastic over thermoset material can be noted here in that the rigidization process begins from the spacecraft end as soon as the deployment begins unlike the thermoset material where the entire structure must be deployed before rigidization can begin. This latter situation is

liable to form wrinkles unless the inflation pressure is kept sufficiently high.

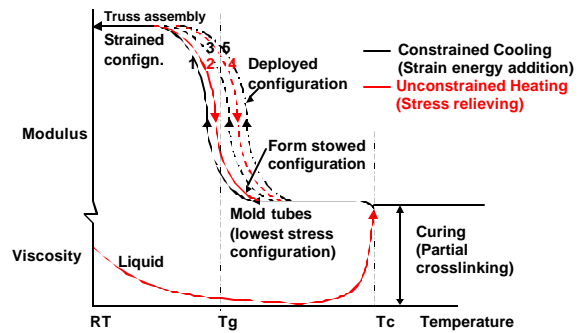


Figure 5 Formation and deployment using a thermoplastic matrix

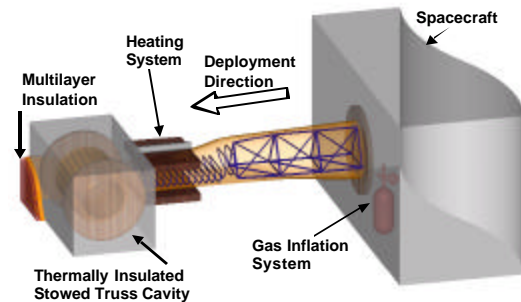


Figure 6 Truss deployment scheme

It is noted here that in this entire process of deployment timing and coordination among several events are of essence. The time to become fully rigid in the desired shape must be rapid so that the impact of the disturbing forces can be minimized. Based on the expected orbital conditions, the time to cool can be tailored by controlling the thermal properties of the shell. Shell material must also be amenable to maintaining the required thermal profile of the structure once deployed. Several alternative methods of in-space rigidization are available for consideration; these include active heating using embedded heaters and passive heating using the solar radiation. The final approach to heating and deploying the truss frame structure can be tailored to fit the requirements of each application.

Potential Impact of Packaging and Deployment

The primary impact on the structural performance of the truss frame is expected

to be from packaging of the frame itself. For packaging, the frame must be collapsed and then rolled on to a spool. This could result in bending of the fibers resulting in yielding or even breakage. To understand the potential risks involved one need to see the folded configuration of the inflatable space frame as shown in Figure 7. From this figure it is seen that the longerons which are the primary load bearing elements of the truss do not undergo any bend as they are simply rolled on the spool of desired diameter. The diagonal members, which carry the torsion and shear load, undergo a very gentle bend radius which can be further improved by optimizing the size and the number of bays. The batten members, which are the least critical members of the frame and do not carry any load, are the ones that undergo the most severe bend of 180° .

Even in the case of batten fold it is seen from figure 8 that if the tubes are made from essentially unidirectional fabric none of the fibers are expected to undergo double fold. The breakage or yielding of the fibers during bending, nevertheless, is a complex but critical issue and requires more detailed study. Towards this end, some bench tests were performed which are described later. From the structural point of view the most critical element and perhaps the weakest link in the structure is expected to be the joint. which is also discussed later.

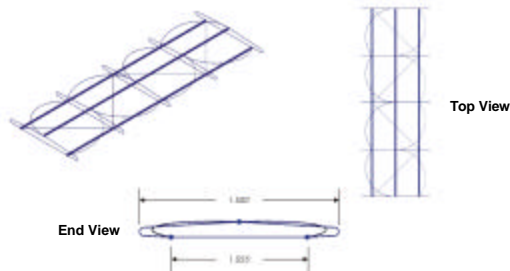


Figure 7 ISF folded configuration

The overall packing technique and the controlled deployment using inflation gas are similar to those exhibited by the monocoque tubular structures on the Inflatable Sunshield In Space (ISIS) program. Therefore, linear deployment with very little off axis migration is expected. Also, the use of inflation gas is expected to result in smooth deployment sequence with low impulse that would minimize the disturbances imparted to the spacecraft.

Potential causes for the structural performance degradation could occur if the structure does not fully form its shape during the deployment. This can occur if the outer shell does not properly tension the structure, or if the shape memory strain does not provide the required forcing function to overcome the local residual stiffness. These issues can be addressed with further characterization of the process and the materials.

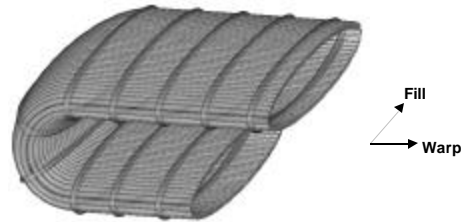


Figure 8 Tube folding characteristics

Design Analysis

Design Methodology

As mentioned before, design of the truss structure is based on the optimization methodology developed by Mikulas [1] with some modifications. These modifications include the fact that the truss application considered here requires cantilever end conditions as opposed to simply supported or hinged beam considered by Mikulas. Another difference was that a single diagonal member was considered instead of cross diagonals. And the third change was that batten members were added. The first change requires that the maximum bending moment occur at the fixed end. The load on the diagonals was doubled to reflect the fact that only single diagonals are used. They are sized for an induced shear load from an assumed lateral imperfection of the column. This results in somewhat overdesign, since ideally the diagonals carry no load. However, this approach provides a mechanism by which the imperfection can rationally be related to either a fabrication process or deformations due to thermal distortions or to lateral acceleration. The batten members, which carry no load, are made identical to the diagonal members for ease in fabrication. The longerons in between the joints are simply supported and are assumed to fail locally by Euler buckling.

Thus, an optimum design would occur when the Euler load for buckling of the longeron section would be equal to the applied compressive loading. The compressive loading includes direct compression and load due to maximum bending moment at the base. For the present case, bending due to any lateral loading is ignored. For an assumed bay number and the diagonal angle the radius of the longerons was determined. Minimizing the total mass then optimizes the number of bays. This methodology was applied for different diagonal angles and length of the truss structure to come up with the potential design points.

Design Tradeoff Study

A composite material of wall thickness 0.381 mm (0.015 in) and a modulus of elasticity of 51.7 Gpa (7.5 Msi) was base lined for the design point selection. Also, the design axial load was assumed to be 2224 N (500 lbf). Four design points are shown in Table 1.

In this table, the first three design points are based on the axial loading of 2250 N and they show the effect of varying the length of the truss and the angle of the diagonal. The design points II and III result in very large equivalent column radius, which was considered impractical for

point I), which gave reasonable equivalent column radius and the length of the truss members. This gives an L/D ratio of 14, which is considered reasonable for highly loaded truss structures. The predicted structural efficiency was $0.03 \text{ kg/m}^{5/3}$. It is of interest here to note that, in the load range under consideration, the optimum truss frame structure requires the diagonal and batten members' diameter so small that it leads to a solid rod cross-section. This significantly challenged the currently available fabrication process. Thus, the design was limited to the smallest fabricable diameter tubes.

Impact of Boom Imperfection

Imperfections in a boom can arise due to a number of reasons, which include manufacturing, thermal gradients and lateral accelerations. This imperfection is represented as the eccentricity of the load applied in the case of a cantilevered boom as shown in Figure 9. The maximum stress, which occurs at the fixed end, is amplified as the applied load approaches the buckling load. In the case of simply supported boom the maximum stress occurs at the center of the boom. The two cases are compared in Figure 10. It is seen that in the case of the simply supported boom the maximum stress rises rapidly at applied loads greater than 60% of the critical buckling load. This limits

Table 1 Design point selection

Design Point	Axial Load N	Design Boom Length m	Number of Bays	Longn. Radius m	Diag. Radius m	Diag. Angle	Equiv. Column Radius m	L/D	Structure Efficiency $\text{kg/m}^{5/3}$
I	2250	5	16	0.005	0.0008	45	0.18	14	0.03
II	2250	60	30	0.0174	0.0029	45	1.2	25	0.023
III	2250	60	21	0.0223	0.0032	60	0.95	32	0.027
IV	500	60	31	0.0106	0.0015	60	0.65	46	0.013

handling given the requirements of the current project. The design point IV, therefore, was added at a lower loading. It reduced the equivalent column radius; however, the length of the diagonal member was beyond the capacity of the currently available oven for curing. It was then decided to design a 5 m long truss (design

the applied load to a much lower value than the critical buckling load to provide sufficient factor of safety. In the case of the cantilever boom the rise in the stress is not as dramatic as the applied load is increased. This can be understood by the fact that P_{cr} for the cantilever boom is $1/4^{\text{th}}$ of that for the boom with simple end supports, or in other

words, for the same load and length cantilever boom must be four times stiffer. Thus, minimizing the effect of imperfection for the cantilever booms.

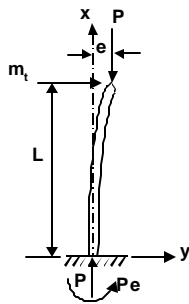


Table 9 Boom imperfection nomenclature

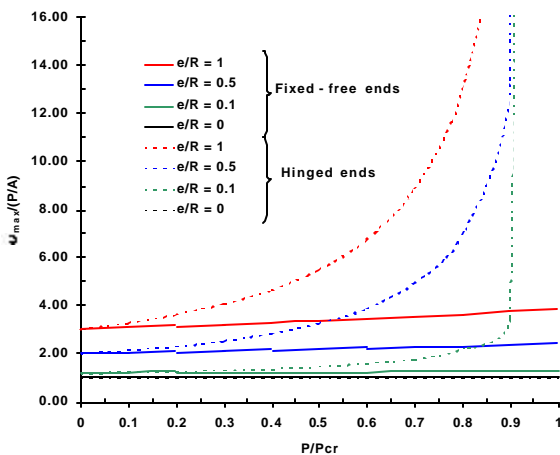


Figure 10 Maximum stress due to boom imperfection

Impact of Boom L/D Ratio

It is clear from the previous discussion that in order to minimize the required factor of safety the column eccentricity must be minimized. From the manufacturing stand point this is practically accomplished in columns, which have a L/D ratio of 100 to 150. On the other hand, large L/D ratio is desirable to achieve minimum mass columns when the column length becomes very large. The impact of Euler loading on the L/D ratio is shown in Figure 11. It is seen from this figure that the practical limits of the L/D ratio determines the minimum Euler design load; which could limit the extent of the optimization. One other trend can be discerned from the figure. This is the fact that the L/D ratio becomes relatively insensitive to the Euler buckling load greater than about 500N for the case shown. This ratio is less than 25 due to the

large diameter requirement. In general it is also true that the L/D ratio is smaller for the cantilever column than for the hinged column. Thus, a truss column can be designed for a lower load without exceeding the practical limit of the L/D ratio. Also, the truss design is not constrained by the r/t ratio, which is typically a constraining parameter on large diameter tubes, which are vulnerable to circumferential buckling. Smaller L/D ratio also has the benefit that it leads to higher frequency.



Figure 11 Impact of compressive loading on L/D ratio

Fabrication

Fabric Selection and Prepregging

The fabric selection was primarily driven by the ability to manufacture the tubes in small diameter sizes and the desire for attaining the highest mechanical properties possible. Other considerations involved were ability to fold the structure for stowage. Whereas, the first requirement primarily dictates the fiber selection, the second requirement affects the selection of the resin. The problems related with the design of foldable structures with self-rigidization are somewhat unique. On one hand the structure must be built with good mechanical properties requiring the designer to select the best weave pattern and laminating procedure. On the other hand, the structure must lose its high modulus properties and become flexible enough to fold at some temperature greater than its normal operating temperature. These two design goals, thus, require proper balancing. For example, a structure built for flexibility at elevated temperature to fold well may not

have the required mechanical stiffness at the lower operating temperature. Considerable amount of effort was expended in arriving at this compromise by conducting several bench top tests in selecting the proper resin content and the fabric weave. As discussed before, the selection of the graphite fiber for the fabric was primarily due to the stiffness requirement. The calculated volume fraction based on the vendor data and the measured volume fraction are compared in Figure 12 and were found to be very close.

It is further noted that this volume fraction is relatively small. Typically a fiber volume fraction of 60% is desirable to achieve the maximum stiffness. The fiber volume fraction in the tubes was deliberately kept low, as mentioned earlier, in order to achieve the foldability. Based on the longitudinal modulus of the graphite fibers and the fiber volume fraction the theoretical longitudinal modulus of the composite material was calculated to be 60.7 Gpa (8.8 Msi) for the two ply prepreg used in 1/2 inch diameter longerons.

<u>Vendor Data</u>	<u>Measured Data</u>
• 17X6 count fabric	• Area of prepreg = 42.25 in ² (.02725 m ²)
• Weight = 5.15oz/yd ²	• Volume of prepreg = 7.616X10 ⁻⁶ m ³
• Thickness = 0.011 in	• Avg. cured mass of prepreg = 7.15 g
• Density of carbon = 1.76 g/cc	• Density of prepreg = 0.94 g/cc
• Calculated V _f = 0.355	• Measured V _f = 0.356

Figure 12 Calculated and measured volume fractions

Bending and Shape memory effect of the Tubes and Joints

It was noted earlier that the warp fibers in small diameter tubes used in the battens undergo the most severe bend of 180°. Some simple bending and shape memory effect tests were performed to establish the processing parameters and demonstrate the principle. Results of a 1/8 in 2-ply tube before, after heating to greater than T_g and folding and after reheating are shown in Figure 13. No fiber damage or seam separation was observed. Lessons learned during the testing indicated that the damage caused is directly related to the angle of the bend. Smaller angle results in less damage. When the fibers do fail, they consistently break in compression (on the inside of the bend).

The individual truss members are joined at their intersection. Ideally it would be desirable to have continuous longerons to which the batten and the diagonal members are joined, as it would significantly improve the reliability of the joints. Because of the limitation on the size of the longeron that can be easily fabricated with the existing tooling and accommodated in the available oven, it was decided to make the longerons of one bay length. These longeron sections were then connected at the intersection with the other members by inserting them into a preformed joint and bonding them using an adhesive. An attempt was made to butt the longeron sections against each other, but there is no assurance that this was actually achieved.

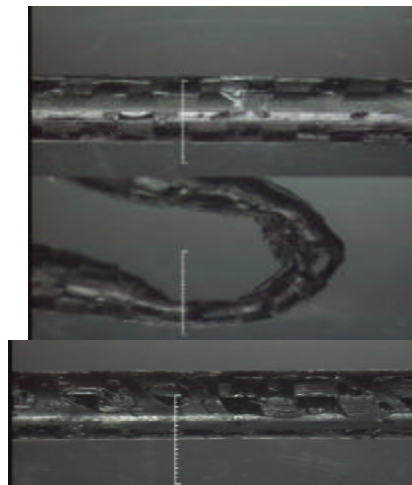


Figure 13 1/8th-inch 2-ply tube bending test

The shearing strength of the longeron joint section was determined by tensile testing and was an average 431 N (97 lbs.). Since no baseline criteria was available it was deemed sufficient for the first truss build up. Based on the truss test results obtained subsequently, it is realized that either this strength must increase substantially or more preferably the longerons must be continuous elements of the truss.

The shape memory is permanently assigned to the joint during the molding process. In order to establish the bending and the shape memory effect of the joint to a first order, a sample joint was fabricated with members bonded with adhesive and was flattened in an oven. It returned to its original

shape upon reheating above the T_g without damage. The sequence of events, before and after packaging, is shown in Figure 14.

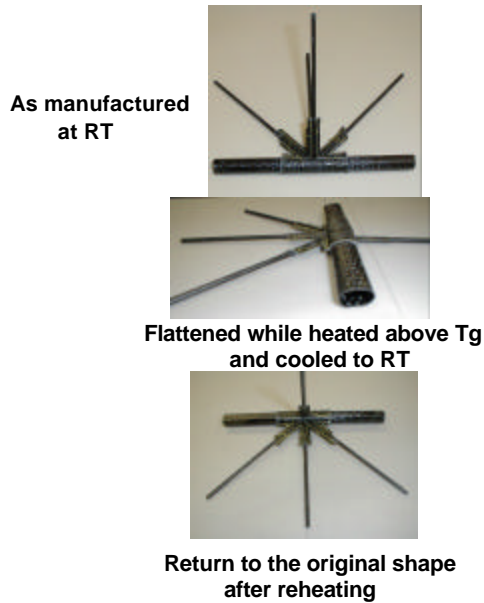


Figure 14 Shape memory effect of a joint

Frame Assembly

Maintaining the dimensional accuracy and alignment were the key requirements during the frame assembly. Any misalignment could degrade the performance, although, as discussed earlier, cantilever column is less susceptible to misalignment than a simply supported column. Further, as the members are bonded together, care was taken to make sure they are not subjected to preloading. Each bay was visually inspected for flatness along the sides and for joint integrity. A shortcoming of the procedure was that once the individual bays were bonded together, one could not test for the quality of the bond. A technique needs to be developed to fix the bond after it is cured. This was found especially critical for the longerons. In any case, an extremely tight alignment (a/l ratio of 0.001) over the entire length of the truss frame was achieved. This was the goal on which the design analysis was based.

Prior to assembly, the mass of the individual members of the assembly was determined. This mass breakdown is shown in Figure 15. It is noted in this figure that longerons contribute about 57% of the total mass. As the longerons are the primary load

bearing elements, for good structural efficiency, they must contribute the largest mass to the overall structure. Diagonal members carry some torsional and shear loading and they are the second highest contributors to the overall mass. The rest of the mass is essentially a parasitic mass, which must be minimized. It is of interest here to note that the total mass in the joints is about 15.8% of the remaining truss mass. This number is very close to that assumed by Mikulas [1] and in the present analysis.

Before Assembly

	Average Mass, g	Total Mass, g	% Mass
Longeron(48)	6.87	329.76	0.573
Diagonal (48)	2.00	96.00	0.167
Batten (48)	1.48	71.04	0.123
Joint (42)	1.71	71.82	0.125
End joint (6)	1.12	6.72	0.012

Total 575.34 g

After Assembly

600.00 g

Figure 15 Truss assembly mass breakdown

The total mass of the truss prior to assembly is 575.34 g and after the assembly it is 600.00 g. The difference is in the adhesive used to assemble the truss. Based on this mass estimate and the length of the truss assembly the structural efficiency parameter is calculated to be $0.04 \text{ kg/m}^{5/3}$. This efficiency parameter is higher than the design point parameter. Primary reason for this is that the tube sizes for the actual frame constructed were larger than those determined based on the optimum design. An additional reason is that the mass of the adhesive was not applied to the calculations.

Testing

The primary objective of the test was to compare the performance of the space frame structure relative to the state-of-the-art structures utilizing the efficiency parameter developed by Mikulas [1]. For this, the modulus of elasticity of the truss assembly and the buckling load at failure were determined. Another objective of the test was to establish the mode of failure. The mounted test setup is shown in Figure 16. From the load vs. deflection curve, the calculated modulus of elasticity was 4.93 Gpa (0.715 Msi). This modulus of elasticity is considerably lower than the theoretically

calculated value of 60.7 Gpa (8.8 Msi). This is directly traced to the longerons not being continuous and joined by a pliable adhesive. Gaps between the sections of the longerons may have further contributed to lowering of the modulus of elasticity.

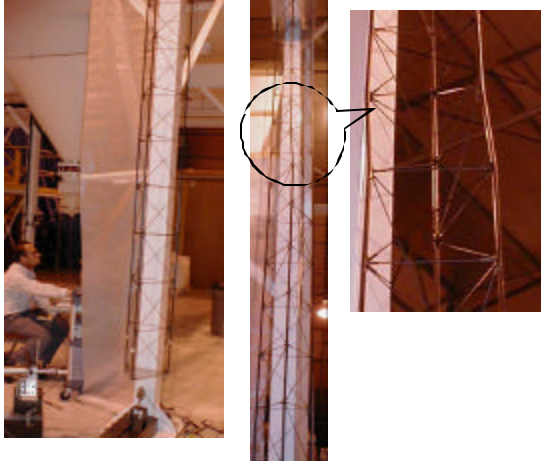


Figure 16 Truss structure test setup and failure mode

It was observed that the truss column buckled locally at around 160-lbf (712 N). The failure point was seen to be located at the joint between the 6th and the 7th bay. This is also shown in Figure 16. The failure point was highly localized as the rest of the column was in extremely good shape. This led to the possibility that this particular joint was defective to begin with and the failure mode is due to potential manufacturing shortcomings. The failure mode was not Euler buckling, which is typically characterized by bowing of the column. The test point is shown against this failure load on the comparative chart in Figure 17.

Conclusions

Overall technical viability of the space frame truss structure was established to first order. Its performance against other space structures indicated that, even with the first attempt, performance comparable to or better than the state-of-the-art concepts was achieved. The shortcoming from the design point was directly traced to the manufacturing process utilized. Thus, performance close to the design point can be expected with the improvement in the manufacturing process. The primary failure mode was localized at the joints, which were considered to be the weakest links in the entire structure. Ways to overcome this weak link have been identified. The size of the structure and potential complexity of heating and deploying at ground level prevented testing of the entire structure. However, the shape memory effect to achieve the foldability/deployability, was demonstrated at the truss element level. It was further established that prevention of damage to the structure during folding requires a delicate balance between the stiffness of the individual elements and the foldability.

References

- [1] Mikulas, M.M., Jr., "Structural Efficiency of Long Lightly Loaded Truss and Isogrid Columns for Space Applications", NASA Technical Memorandum 78687, July 1978.
- [2] Darooka, D.K., S. Scarborough, S. Malghan, D. Cadogan, C. Knoll, "Inflatable Space Frame", Final Report, NASA Prime Contract Number: NAS1-99154, July 2000.

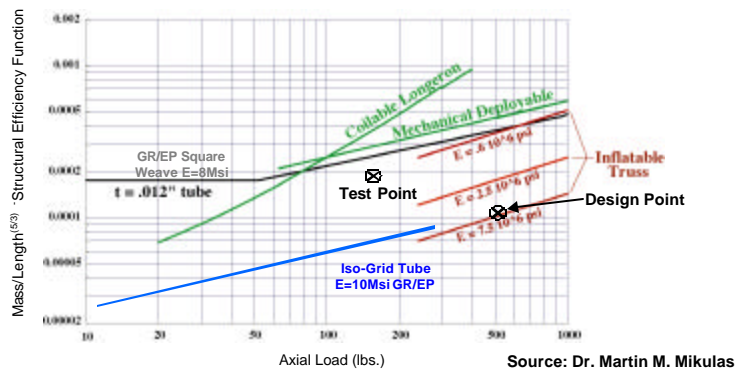


Figure 17 Comparison with other column designs